nature chemical biology

© 2006 Nature Publishing Group http://www.nature.com/naturechemicalbiology

Sulfation patterns of glycosaminoglycans encode molecular recognition and activity

Cristal I Gama[1,5], Sarah E Tully[1,5], Naoki Sotogaku[2], Peter M Clark[1], Manish Rawat[1], Nagarajan Vaidehi[3,4], William A Goddard III[3], Akinori Nishi[2] & Linda C Hsieh-Wilson[1]

Although glycosaminoglycans contribute to diverse physiological processes[1–4], an understanding of their molecular mechanisms has been hampered by the inability to access homogeneous glycosaminoglycan structures. Here, we assembled well-defined chondroitin sulfate oligosaccharides using a convergent, synthetic approach that permits installation of sulfate groups at precise positions along the carbohydrate backbone. Using these defined structures, we demonstrate that specific sulfation motifs function as molecular recognition elements for growth factors and modulate neuronal growth. These results provide both fundamental insights into the role of sulfation and direct evidence for a 'sulfation code' whereby glycosaminoglycans encode functional information in a sequence-specific manner analogous to that of DNA, RNA and proteins.

Glycosaminoglycans have an inherent capacity to encode functional information that rivals DNA, RNA and proteins. Specifically, these polysaccharides show diverse patterns of sulfation that are tightly regulated *in vivo*[5,6]. Over the past several decades, genetic and biochemical studies have established the importance of glycosaminoglycans in regulating many physiological processes, including morphogenesis and development, viral invasion, cancer metastasis and spinal cord injury[1–4]. However, a key unresolved question is whether glycosaminoglycans use specific sulfation sequences to modulate biological processes.

Advancing a molecular-level understanding of glycosaminoglycans will require new tools for studying their structure-function relationships. Although several strategies have been developed, there are currently no methods to explore systematically the role of specific sulfation sequences. For instance, genetic approaches that target a particular sulfotransferase gene perturb many sulfation patterns throughout the polysaccharide chain and therefore cannot be used to study the impact of a single structural motif[1,7]. Biochemical methods afford a mixture of heterogeneously sulfated compounds of poorly defined linear sequence[8], thereby complicating efforts to relate a biological function to a specific sulfation sequence. We reasoned that chemical synthesis could provide a powerful means to access well-defined structures and enable systematic investigations into the role of sulfation. Here, we describe such an approach and provide evidence that chondroitin sulfate (CS) glycosaminoglycans encode functional information in a sequence-specific manner.

We used chemical synthesis to generate oligosaccharides representing three important subclasses of CS found *in vivo* (**Scheme 1**). Tetrasulfated compound **1** shows the CS-E sulfation sequence, a motif that is enriched in the developing brain[9,10] and associated with the proteoglycans appican, syndecan-1, syndecan-4, neuroglycan C and phosphacan[10–12]. Disulfated compounds **2** and **3** represent the most abundant sulfation patterns *in vivo*, CS-C and CS-A, respectively[9]. For comparison, we also synthesized tetrasulfated oligosaccharide **4**, denoted CS-R, which possesses the same overall negative charge as **1** but has sulfate groups installed at the C2 and C3 positions of D-glucuronic acid (GlcA).

The synthesis of glycosaminoglycans is notoriously challenging; historically, more than 40 chemical steps have been required to create a single oligosaccharide[13]. Their construction necessitates stereospecific formation of α- and β-glycosidic linkages, use of uronic acid donors or acceptors having low reactivity, and regiospecific functionalization of hydroxyl groups having similar reactivity to install distinct sulfation sequences. To be practical for biological studies, a modular, efficient approach must be designed to minimize the number of steps and afford sufficient quantities of oligosaccharides for analysis. Our synthetic route allows for the generation of various CS sulfation motifs from a core disaccharide building block, **5**. We achieved stereocontrol in the glycosylation reactions to form β-linked oligosaccharides using α-trichloroacetimidate donors containing C2 *N*-trichloroacetyl (TCA) or *O*-benzoyl (Bz) participating groups. We developed an orthogonal protecting-group strategy to install the specific sulfation sequences. In particular, we used *p*-methoxybenzylidene and Bz groups to mask positions that were exposed for sulfation at late stages of the synthesis. To elongate the carbohydrate chain, we used a silyl ether to protect the C4 position of GlcA and liberate a hydroxyl-group nucleophile for reaction with a glycosylating agent. Finally, we appended a versatile chemical handle, the allyl moiety, to

[1]Division of Chemistry and Chemical Engineering and Howard Hughes Medical Institute, California Institute of Technology, Pasadena, California 91125, USA. [2]Department of Pharmacology, Kurume University School of Medicine, 67 Asahi-machi, Kurume, Fukuoka 830-0011, Japan. [3]Materials and Process Simulation Center (MSC), California Institute of Technology, Pasadena, California 91125, USA. [4]Present address: Division of Immunology, City of Hope Cancer Research Center, Beckman Research Institute of City of Hope, 1500 East Duarte Road, Duarte, California 91010, USA. [5]These authors contributed equally to this work. Correspondence should be addressed to L.C.H.-W. (lhw@caltech.edu).

Received 24 March; accepted 6 July; published online 30 July 2006; doi:10.1038/nchembio810

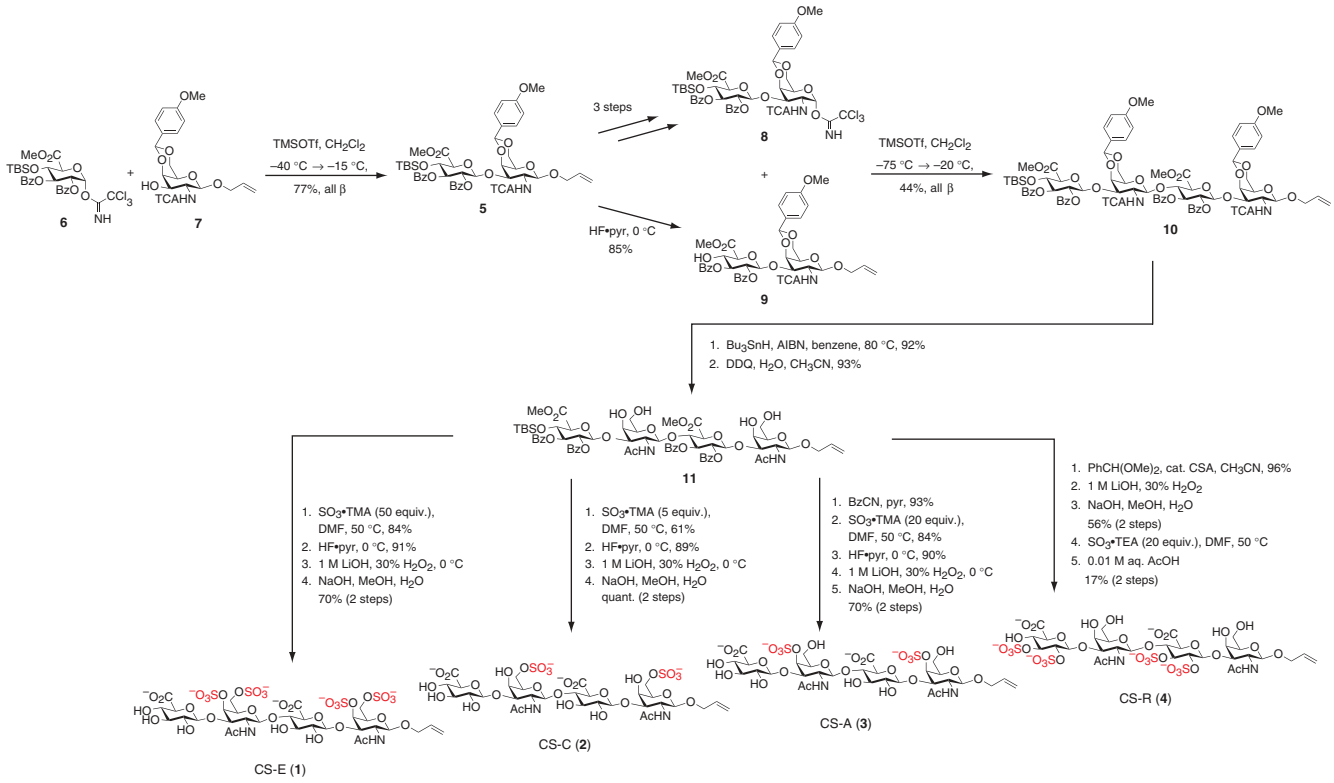

Scheme 1 Synthesis of CS tetrasaccharides of defined sulfation pattern, stereochemistry and chain length. We assembled tetrasaccharides from a core disaccharide building block, **5**, and elaborated them to install distinct sulfation motifs. This modular, convergent approach permits access to a variety of sulfation patterns, including three important sulfation motifs found in the mammalian brain (CS-E, CS-C and CS-A) and the CS-R motif, which has the same overall electrostatic charge as CS-E and can be used to evaluate further the importance of sulfate group orientation. TMSOTf, trimethylsilyl trifluoromethansulfonate; CH_2Cl_2, dichloromethane; HF•pyr, hydrogen fluoride–pyridine complex; Bu_3SnH, tri-*n*-butyltin hydride; AIBN, 2,2'-azobisisobutyronitrile; DDQ, 2,3-dichloro-5,6-dicyano-1,4-benzoquinone; H_2O, water; CH_3CN, acetonitrile; SO_3•TMA, sulfur trioxide–trimethylamine complex; DMF, dimethylformamide; LiOH, lithium hydroxide; H_2O_2, hydrogen peroxide; NaOH, sodium hydroxide; MeOH, methanol; BzCN, benzoyl cyanide; pyr, pyridine; $PhCH(OMe)_2$, benzaldehyde dimethyl acetal; CSA, DL-10-camphorsulfonic acid; SO_3•TEA, sulfur trioxide–triethylamine complex; AcOH, acetic acid; TBS, *t*-butyldimethylsilyl; Bz, benzoyl; TCA, trichloroacetyl; Me, methyl; Ac, acetyl.

the reducing end of the oligosaccharides for convenient conjugation to proteins, small molecules and surfaces.

We synthesized the core disaccharide building block on a multigram scale from protected monosaccharides **6** and **7** (ref. 14). For elongation of the carbohydrate chain, the disaccharide was readily converted to a suitable glycosyl donor and acceptor pair (**8** and **9**). Silyl deprotection of **5** using hydrogen fluoride–pyridine complex to yield **9**, followed by coupling to activated imidate **8**, produced the β-linked tetrasaccharide **10** with excellent stereoselectivity.

With an efficient route to the tetrasaccharide, we next focused on the assembly of CS structures bearing distinct sulfation motifs. Radical-mediated conversion of the TCA to an *N*-acetyl group and oxidative cleavage of the *p*-methoxybenzylidene acetal afforded the key tetraol intermediate **11**. Sulfation of **11** under vigorous conditions generated the precursor to CS-E and under mild conditions yielded the precursor to CS-C. We obtained the target CS-E and CS-C tetrasaccharides (**1** and **2**, respectively) after silyl deprotection and saponification. We synthesized the CS-A tetrasaccharide **3** by selectively benzoylating the C6 hydroxyl groups using benzoyl cyanide[15] and then sulfating at the C4 position. We removed the remaining silyl and ester protecting groups as described above to afford **3**. Finally, tetrasulfated **4** was generated through formation of the benzylidene acetal, which proved more stable than the *p*-methoxybenzylidene acetal during the sulfation reaction. After saponification, the resulting free hydroxyl groups were sulfated and the desired CS-R tetrasaccharide obtained after deprotection of the remaining protecting groups under mildly acidic conditions. We purified tetrasaccharides **1**, **2**, **3** and **4** by size-exclusion chromatography and confirmed their structures by ^{1}H-NMR, proton decoupling experiments and ESI-MS.

With the ability to access well-defined CS sequences, we embarked on systematic investigations into the role of sulfation. Heparan sulfate and CS glycosaminoglycans play critical roles in cell growth and development by regulating various growth factors, including fibroblast growth factors (FGFs), Hedgehog, Wingless and semaphorins[1,16,17]. The structural diversity of glycosaminoglycans *in vivo* has led to the hypothesis that specific sulfated structures may modulate the binding and activity of growth factors. However, the complexity and heterogeneity of glycosaminoglycans have hindered efforts to establish whether growth factors recognize unique sulfation sequences. We first investigated computationally whether subtle variations in the sulfation pattern would favor distinct structural conformations of glycosaminoglycans. Here we used the Dreiding force field[18] (modified slightly using quantum mechanics; see Methods) with charges from the charge equilibrium[19] (QEq) method and carried out Boltzmann jump simulations[20] on tetrasaccharides **1**, **2**, **3** and **4** to obtain the lowest-energy CS conformations. We then used these conformations to perform molecular dynamics simulations[20] in explicit water to predict the optimum conformation in solution. We found that each

© 2006 Nature Publishing Group http://www.nature.com/naturechemicalbiology

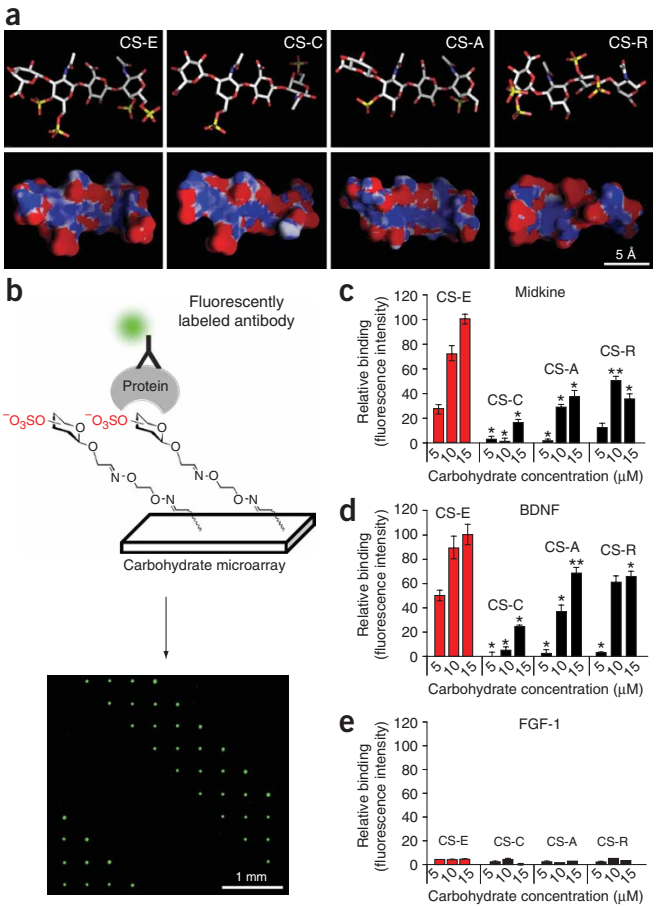

Figure 1 A specific sulfation pattern promotes the interaction of CS with neuronal growth factors. (**a**) Average structures from molecular dynamics simulations of the CS tetrasaccharides in water. The sulfation pattern influences the structure of CS, allowing it to present distinct electrostatic and van der Waals surfaces to proteins. We generated the CS ball-and-stick figures in PyMOL (DeLano Scientific) and created the electrostatic maps using GRASP (available online at http://trantor.bioc.columbia.edu/grasp/). (**b**) Overall scheme to detect CS-protein interactions using carbohydrate microarrays. Each microarray contained 1,000 spots; a representative portion of the microarray after binding to the CS-C antibody is shown. See **Supplementary Figure 5** for a description of the spotting pattern. (**c**,**d**) The CS-E tetrasaccharide interacts with the growth factors midkine (**c**) and BDNF (**d**). Altering the position of the sulfate groups, but not the overall electrostatic charge, modulates the binding interaction. Each bar (mean ± s.e.m.) represents an average of 5–10 spots. (**e**) None of the CS tetrasaccharides interact with FGF-1. We compared binding data for FGF-1 to the average fluorescence intensity obtained for midkine binding to 15 μM CS-E. We performed all statistical analyses using the one-way ANOVA followed by the Scheffe test; $n \geq 5$. $^{*}P < 0.0001$, relative to CS-E tetrasaccharide for a given concentration. $^{**}P \leq 0.001$, relative to CS-E tetrasaccharide for a given concentration.

CS tetrasaccharide favors a distinct set of torsion angles and presents a unique electrostatic and van der Waals surface for interaction with proteins (**Fig. 1a** and **Supplementary Figs. 1–4** online). Whereas the negatively charged sulfate and carboxylate groups on CS-C point toward either the top or bottom face of the molecule, as oriented in **Figure 1a**, the same charges on CS-A point in several different directions. Similarly, although CS-E and CS-R have the same number of sulfate groups, the relative orientation of these groups along the carbohydrate backbone leads to distinctly different predicted solution structures. Whereas the CS-R tetrasaccharide has the sulfate groups distributed along several faces of the molecule, the CS-E tetrasaccharide presents all four sulfate groups along a single face, which may position the groups to interact with basic residues characteristic of glycosaminoglycan binding sites on proteins[2].

To explore the functional consequences of sulfation on growth factor binding, we used tetrasaccharides **1**, **2**, **3** and **4** to construct carbohydrate microarrays. Carbohydrate microarrays have proven to be powerful tools for investigating the interactions of various glycans with proteins, viruses and bacteria[21–23]. However, they have not been extensively exploited for detailed structure-function analyses of glycosaminoglycans, whose structures differ only subtly in their sulfation pattern and are identical in stereochemistry and sugar composition. The potential of microarrays to distinguish such closely related structures has been unclear, as most studies have used carbohydrates of very different composition, such as mannose versus galactose or tetrasaccharides versus hexasaccharides[21–23]. To fabricate the microarrays, we appended an aminooxy linker to the reducing end of tetrasaccharides **1**, **2**, **3** and **4** by ozonolysis of the allyl group and reaction with 1,2-(bisaminooxy)ethane. This linker enabled immobilization of the oligosaccharides on aldehyde-coated slides via formation of a covalent oxime bond. We used a high-precision contact-printing robot to deliver nanoliter volumes of the compounds to aldehyde-coated slides, yielding 1,000 spots approximately 200 μm in diameter (**Fig. 1b**). We washed the slides before using them and quenched the unreacted aldehyde moieties on the slide surfaces using $NaBH_4$. We validated the methodology by probing the microarrays initially with a mouse monoclonal antibody selective for the CS-C sulfation motif (**Supplementary Methods** online). We visualized the binding of antibodies to the tetrasaccharides using a secondary Cy3-conjugated goat anti-mouse antibody. The CS-C antibody bound to the CS-C tetrasaccharide in a concentration-dependent manner, and we observed selectivity of this antibody for the CS-C motif with no detectable binding to the CS-A, CS-E or CS-R tetrasaccharides (**Supplementary Fig. 5** online).

Having validated the microarray methodology, we investigated the effects of sulfation on the binding of CS to the growth factor midkine. Midkine participates in the development and repair of neural and other tissues[24] and binds with nanomolar affinity to heterogeneous polysaccharides enriched in the CS-E motif[9]. We observed selective binding of midkine to the CS-E tetrasaccharide at CS concentrations within the physiological range[25]. Notably, the midkine interaction was highly sensitive to the position of the sulfate groups along the carbohydrate backbone (**Fig. 1c**). The interaction of midkine with CS-A and CS-C, the most abundant sulfation motifs in the mammalian brain[9], was significantly weaker than that with CS-E ($P < 0.0001$). Midkine also did not interact as strongly with CS-R as with CS-E, indicating that the midkine-CS association requires a specific arrangement of sulfate groups and is not governed by nonspecific, electrostatic interactions.

Access to defined sulfation sequences coupled with microarray technologies provides a powerful, rapid means to identify new glycosaminoglycan-protein interactions and to gain insight into the functions of specific sulfation sequences. In addition to midkine, we discovered that brain-derived neurotrophic factor (BDNF) selectively binds to the CS-E sulfation sequence. The neurotrophin BDNF controls many aspects of mammalian nervous system development and contributes to synaptic plasticity, neurotransmission and neurodegenerative disease[26]. We found that BDNF has a 20-fold preference for the CS-E motif relative to those of CS-C, CS-A and CS-R at

© 2006 Nature Publishing Group http://www.nature.com/naturechemicalbiology

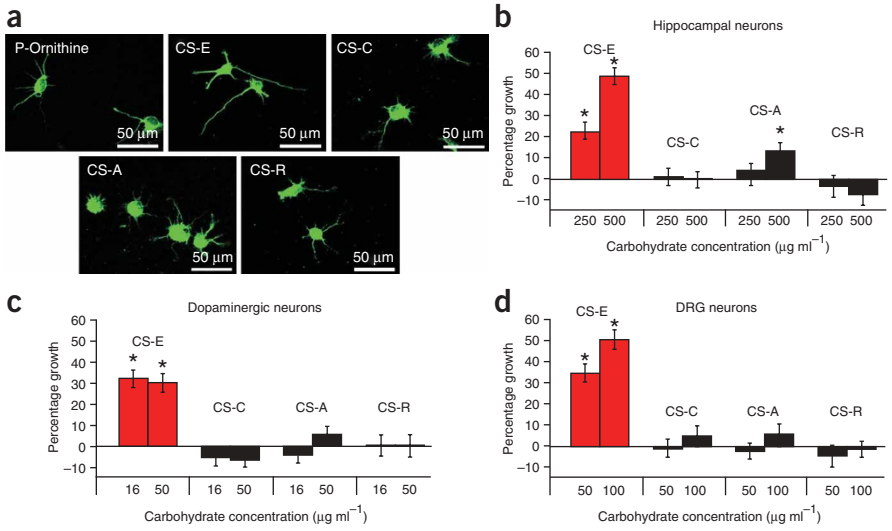

Figure 2 The sulfation pattern directs the neuritogenic activity of CS. (**a**) Representative immunofluorescence images of hippocampal neurons cultured on a substratum of polyornithine and the synthetic tetrasaccharides. Scale bar, 50 μm. (**b**) The CS-E tetrasaccharide **1** stimulates the outgrowth of hippocampal neurons. Altering the position of the sulfate groups, but not the overall electrostatic charge, modulates the neuritogenic activity of CS. (**c**,**d**) The specific sulfation pattern directs the activity of CS toward various neuron types. The CS-E tetrasaccharide **1** promotes the outgrowth of dopaminergic (**c**) and DRG (**d**) neurons. We cultured neurons for 2–5 d on glass coverslips coated with polyornithine and the tetrasaccharides at the indicated concentrations. We quantified neurite length (mean ± s.e.m.), expressed as percentage growth relative to polyornithine control, using NIH Image 1.62 (available online at http://rsb.info.nih.gov/nih-image) or Neurolucida 2000 (MicroBrightField Inc.) software after immunostaining with antibodies to tubulin (**a**,**b**), tyrosine hydroxylase (**c**) or β-tubulin III (**d**). We performed statistical analysis using the one-way ANOVA followed by the Scheffe test; $n = 50$–200 cells. $^*P < 0.0001$, relative to polyornithine control.

5 μM CS, which approximates the estimated concentration of CS-E present in physiological samples[9,10,25] (**Fig. 1d**). As a control, we demonstrated that none of the tetrasaccharides interacts strongly with FGF-1 (**Fig. 1e**), which is consistent with studies indicating that FGF-1 is regulated by heparan sulfate but not by CS glycosaminoglycans[8,16].

Having shown that distinct sulfation sequences can modulate the interactions of CS with specific growth factors, we next investigated the impact of sulfation on cell growth. As both midkine and BDNF stimulate neuronal outgrowth, we compared the neuritogenic activity of tetrasaccharides **1**, **2**, **3** and **4**. We cultured primary hippocampal neurons from embryonic day 18 (E18) rats on coverslips coated with polyornithine and each of the four compounds. After 48 h, we fixed the neurons, immunostained them with antibodies to tubulin and examined them by confocal fluorescence microscopy. A specific CS sulfation pattern was required for the growth-promoting activity of CS. Whereas the CS-E tetrasaccharide stimulated neurite outgrowth by 48.6 ± 2.3% relative to the polyornithine control, tetrasaccharides representing other CS subclasses found *in vivo* (CS-A and CS-C) had no appreciable activity (**Fig. 2a**,**b**). Notably, CS-R had no effect on neurite outgrowth, despite having the same overall negative charge as CS-E. These results are consistent with previous reports that CS polysaccharides enriched in the CS-E sulfation pattern possess neuritogenic activity[8]. In this study, we extend those findings by establishing that a precise orientation of the sulfate groups is critical for the growth-inducing ability of CS.

We next investigated whether the effects of the CS-E motif are unique to specific cell types. Paradoxically, CS has been reported both to stimulate and inhibit neuronal growth, depending on the cellular context. For instance, CS proteoglycans can repel migrating neurons or extending axons during brain development or after injury[4,17]. However, CS staining also coincides with developing axon pathways, and tissues expressing CS do not always exclude axon entry[27]. To examine whether sulfation is important for the growth of other neuron types, we cultured dopaminergic neurons from the mesencephalon of rat embryos on a substratum of each tetrasaccharide. We found that the CS-E tetrasaccharide has similar activity toward both dopaminergic and hippocampal neurons, inducing the outgrowth of dopaminergic neurons by 29.6 ± 6.0% (**Fig. 2c**). In contrast, the CS-C, CS-A and CS-R motifs showed no appreciable neuritogenic activity. Similarly, we observed that the CS-E tetrasaccharide, but not the other sulfation motifs, stimulates the outgrowth of dorsal root ganglion (DRG) neurons derived from the spinal cord (**Fig. 2d**). The ability of the CS-E sulfation motif to elicit a response in various cell types suggests that protein receptors, shared by many cell types, are likely present to engage the sugar. These results indicate that the molecular structure of CS glycosaminoglycans is critical for the function of CS, independent of neuron type.

The ability of the CS-E sulfation sequence to interact with growth factors and modulate neuronal growth suggests that CS may recruit specific growth factors to the cell surface, thereby activating downstream signaling pathways. To investigate this potential mechanism, we cultured hippocampal neurons on a CS-E tetrasaccharide or polyornithine substratum in the presence or absence of antibodies

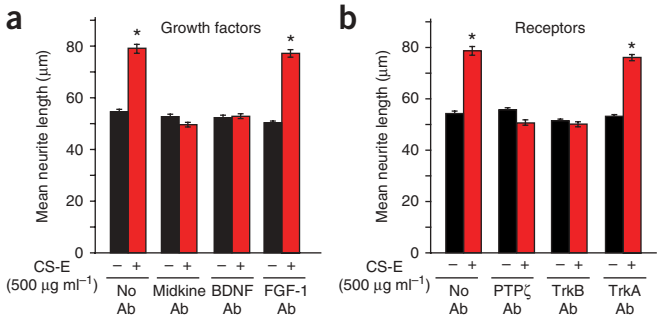

Figure 3 The CS-E sulfation motif stimulates neuronal growth through activation of the midkine-PTPζ and BDNF-TrkB signaling pathways. (**a**) Antibodies (Ab) selective for midkine or BDNF, but not FGF-1, block the neurite outgrowth induced by CS-E. (**b**) Antibodies against the receptors PTPζ or TrkB, but not TrkA, abolish the growth-promoting effects of CS-E. We cultured hippocampal neurons on a substratum of polyornithine or polyornithine plus the CS-E tetrasaccharide. After 24 h, we added the antibodies to the medium and incubated them with the cells for 24 h. We quantified neurite length (mean ± s.e.m.) using NIH Image 1.62 software after immunostaining them with antibodies to tubulin. $^*P < 0.0001$, relative to the CS-E, no-antibody control; $n = 150$ cells.

© 2006 Nature Publishing Group http://www.nature.com/naturechemicalbiology

© 2006 Nature Publishing Group http://www.nature.com/naturechemicalbiology

selective for midkine or BDNF[28,29]. The antibodies were expected to block the interaction of the endogenous growth factors with the CS-E substratum and thereby abolish the neuritogenic effects. We first confirmed that the antibodies could disrupt binding of the growth factors to CS-E using the carbohydrate microarrays. As expected, the antibodies effectively blocked the interaction between midkine or BDNF and the CS-E tetrasaccharide on the microarray (**Supplementary Fig. 6** online). Next we examined the ability of the antibodies to inhibit the neuritogenic effects of CS-E. Antibodies to midkine or BDNF had no effect on neurite outgrowth in the absence of the tetrasaccharide (**Fig. 3a** and **Supplementary Fig. 7** online). Addition of either antibody blocked the neurite outgrowth induced by CS-E. In contrast, neither a control antibody selective for FGF-1 nor class-matched control antibodies could abolish the growth-promoting effects of CS-E (**Fig. 3a** and **Supplementary Fig. 7**).

As further confirmation, we used antibodies that recognize the extracellular domains of the cell surface receptors protein tyrosine phosphatase ζ (PTPζ) and tyrosine kinase B receptor (TrkB). Binding of midkine and BDNF to PTPζ and TrkB, respectively, promotes neuronal outgrowth and survival in various systems by activating intracellular pathways such as the mitogen-associated protein kinase (MAPK) and phosphatidylinositol 3-kinase (PI3-K) pathways[24,26]. Notably, antibodies against either PTPζ or TrkB[28] blocked the neuritogenic activity of CS-E (**Fig. 3b** and **Supplementary Fig. 7**). In contrast, neither antibody alone had an effect on neurite outgrowth in the absence of CS-E. To demonstrate the specificity of the effects, we showed that function-blocking TrkA[30] and class-matched control antibodies do not influence CS-E–mediated neurite outgrowth (**Fig. 3b** and **Supplementary Fig. 7**). These results indicate that the CS-E sulfation motif stimulates neuronal growth through activation of midkine-PTPζ and BDNF-TrkB signaling pathways.

Together, these studies provide compelling support for the existence of a 'sulfation code' whereby the precise position of sulfate groups along the carbohydrate backbone permits glycosaminoglycans to encode information in a sequence-specific manner. Using well-defined oligosaccharides, we have shown directly that distinct CS sulfation sequences can function as molecular recognition elements for growth factors and facilitate activation of associated signaling pathways. Moreover, the activity of CS-E relative to other CS subclasses and CS-R, as well as the preservation of activity across different cell types, suggests the importance of specific molecular interactions rather than nonspecific, electrostatic effects. Heparan sulfate, a related glycosaminoglycan, has also been proposed to operate through a sulfation code[7], and the concept finds strong precedent in the sequence-specific manner in which other biopolymers (DNA, RNA and proteins) interact with their molecular targets.

According to the sulfation code hypothesis, chemical modifications to the polysaccharide backbone may be introduced in a time- or region-specific manner, such as during neuronal development or in response to injury. Precise modifications to glycosaminoglycans could facilitate or inhibit ligand-receptor interactions in a highly localized fashion, providing an exquisite mechanism for regulatory control. Indeed, specific sulfation motifs might control the diffusion and efficient signaling of growth factors, establishing concentration gradients and boundaries. In support of this view, the *tout-velu* gene responsible for heparan sulfate biosynthesis in *Drosophila melanogaster* is required for Hedgehog diffusion during embryonic patterning[31]. Moreover, specific CS sulfation motifs are upregulated during neuronal development and enriched along axon growth tracts[32].

Understanding the roles of glycosaminoglycans will require new approaches and reagents to probe and manipulate their structures. We have shown that chemical approaches are particularly valuable in this regard, enabling identification of biologically active sulfation motifs, systematic structure-function studies and analysis of glycosaminoglycan-protein interactions. Though glycosaminoglycans cannot yet be assembled with the same ease as nucleic acids or proteins, rapid advances in their synthesis and characterization are enabling the first molecular-level investigations of this important class of biopolymers. We anticipate that our approach to systematically explore the role of sulfation sequences will both open numerous opportunities for structural and biophysical studies and facilitate exploration of the roles of glycosaminoglycans across various proteins and biological contexts.

METHODS

Synthesis of CS compounds 1, 2, 3 and 4. See **Supplementary Methods** for experimental procedures and compound characterizations.

Molecular dynamics simulations. For each tetrasaccharide, we assigned charge equilibrium (QEq)[19] charges and generated 1,000 conformations using a Boltzmann jump method with rotation around the glycosidic bonds followed by structural minimization. We sorted the resulting conformations into five groups by root mean square deviation in coordinates and ranked them by their potential energies. We ran 300 ps of explicit water molecular dynamics at 300 K on the two lowest-energy conformations from each of the five groups. For each of the ten molecular dynamics runs, we averaged the tetrasaccharide conformations from the last 100 ps and calculated their potential energies with explicit solvation. We used the lowest-energy structure among these ten to represent the predicted solution structure, and we performed the Boltzmann jumps and the molecular dynamics calculations using Cerius2 (Accelrys Inc.)[20]. We used the Dreiding force field[18], adapted to include sulfate groups, throughout the calculations; we modified the force field by optimizing the bond lengths and angles of a model CH_3OSO_3Na system through quantum mechanics (Jaguar)[33] and adjusting the Dreiding force field parameters based on this optimum geometry.

Carbohydrate microarrays. We arrayed solutions of the aminooxy oligosaccharides in 300 mM NaH_2PO_4, pH 5.0 (10 μl $well^{-1}$ in a 384-well plate) on Hydrogel Aldehyde slides (NoAb Biodiscoveries) by using a Microgrid II arrayer (Biorobotics) to deliver subnanoliter volumes at room temperature (23–25 °C) and 50% humidity. Final concentrations of carbohydrates on the slide ranged from 0 to 500 μM. We selected 25 concentrations and repeated each concentration 10 times for a total of 1,000 spots. We incubated the resulting arrays in a 70% humidity chamber at room temperature overnight and then stored them in a low humidity, dust-free desiccator. Before using the arrays, we outlined them with a hydrophobic pen (Super Pap Pen, Research Products International) to create a boundary for the protein treatments, and then we rinsed them three times with H_2O. We then blocked the slides by treatment with $NaBH_4$ (125 mg) in phosphate-buffered saline (PBS, 50 ml) at room temperature for 5 min and washed them five times with PBS. We added human midkine (Peprotech), BDNF (Peprotech), FGF-1 (R & D Systems; all reconstituted to 2 μM in 0.1% Triton X-100 in PBS) and monoclonal antibody 5D2-2C2 (raised against CS-C) to the slides in 200 μl quantities and incubated them at room temperature for 2 h. We then washed the slides with PBS and incubated them with the appropriate primary antibody (anti-midkine, Peprotech; anti-BDNF, Santa Cruz; anti-FGF-1, R & D Systems; 1:1,000 in 0.1% Triton X-100 in PBS) for 2 h at room temperature. After the incubation, we washed the slides with PBS and treated them in the dark at room temperature with a secondary IgG antibody conjugated to Cy3 (Amersham; 1:5000 in 0.1% Triton X-100 in PBS) for 1 h. We washed the slides with PBS followed by H_2O and then dried them under a gentle stream of N_2. We analyzed microarrays at 532 nm using a GenePix 5000a scanner and quantified fluorescence using GenePix 6.0 software after correcting for local background. We analyzed each protein in triplicate, and the data represent an average of 5–10 spots for a given carbohydrate concentration. For the blocking experiments using midkine and BDNF antibodies, we preincubated recombinant human midkine (Peprotech,

2 μM) and either a goat anti-midkine IgG (Santa Cruz, 5 μM) or a goat anti-mouse IgG (Pierce, 5 μM) in 200 μl of 0.1% Triton X-100 in PBS at room temperature for 2 h. Similarly, we preincubated recombinant human BDNF (Peprotech, 2 μM) and either a rabbit anti-BDNF IgG (Santa Cruz, 5 μM) or a rabbit anti-mouse IgG (Pierce, 5 μM) in 200 μl of 0.1% Triton X-100 in PBS at room temperature for 2 h, and also recombinant human BDNF (Peprotech, 2 μM) and either a chicken anti-BDNF IgY[28,29] (Promega, 5 μM) or a chicken IgY (Promega, 5 μM) in 200 μl of 0.1% Triton X-100 in PBS at room temperature for 2 h. We then treated the carbohydrate microarrays with these solutions at room temperature for 2 h and processed and analyzed them as described above.

Neuronal cultures and neurite outgrowth measurements. We prepared coverslips, cultured hippocampal neurons and measured neurite outgrowth as described previously[14]. We prepared DRG cultures from the spinal cords of E18 embryos of Sprague-Dawley rats. We dissected ganglia in Calcium- and Magnesium-Free Hank's Balanced Salt Solution (CMF-HBSS; Gibco), digested them with 0.25% trypsin (Gibco) for 20 min at 37 °C and dissociated the resulting fragments in culture medium consisting of DMEM-F12 (Gibco), 10% horse serum (Gibco), N2 supplement (Gibco) and nerve growth factor (50 ng ml^{-1}; Gibco). We plated DRG neurons at 100 cells mm^{-2} on coverslips coated with poly-DL-ornithine and the tetrasaccharides (100 μl of a 50 or 100 μg ml^{-1} solution). After 24 h, we immunostained neurons with an antibody to β-tubulin III (Sigma; 1:500) and examined them by confocal fluorescence microscopy. We imaged cells on a Zeiss Axiovert 100M inverted confocal microscope and captured the images with LSM Pascal software. We cultured mesencephalic cells on dishes coated with polyornithine and the tetrasaccharides (100 μl of a 16 or 50 μg ml^{-1} solution) for 5 d, immunostained them with an antibody to tyrosine hydroxylase (Pel-Freeze; 1:1,000) and examined them by confocal fluorescence microscopy. The neurite length is expressed as total length of the neurite from the perikarya, and only cells with neurites longer than one cell body diameter were counted, as per standard protocol. We measured the length of the longest neurite using NIH Image 1.62 software. We compared the mean neurite lengths among the different substrate conditions with the ANOVA test followed by the Scheffe test using the statistical analysis program StatView (SAS Institute Inc.). The animal protocol was approved by the Institutional Animal Care and Use Committee at Caltech, and all procedures were performed in accordance with the Public Health Service Policy on Humane Care and Use of Laboratory Animals.

Antibody treatment of neuronal cultures. For the antibody treatments, we cultured hippocampal neurons on a substratum of poly-DL-ornithine in the presence or absence of CS-E tetrasaccharide (100 μl of a 500 μg ml^{-1} solution). After 24 h, we added to the medium (final volume of 500 μl) antibodies selective for midkine (Santa Cruz; goat IgG raised against the C terminus of the protein; final concentration of 4 μg ml^{-1}), BDNF (Santa Cruz; rabbit IgG raised against residues 130–247; final concentration of 1 μg ml^{-1}; and Promega[28,29]; chicken IgY raised against human recombinant protein; final concentration of 10 μg ml^{-1}), FGF-1 (R & D Systems; mouse IgG raised against recombinant human protein; final concentration of 4 μg ml^{-1}), PTPζ (Santa Cruz; rabbit IgG raised against extracellular domain residues 141–440; final concentration of 2 μg ml^{-1}), TrkB (Santa Cruz; goat IgG raised against the extracellular domain; final concentration of 1 μg ml^{-1}; and BD Transduction Laboratories[29]; mouse IgG raised against extracellular residues 156–322; final concentration of 0.5 μg ml^{-1}), or TrkA (Santa Cruz; goat IgG raised against the extracellular domain; final concentration of 4 μg ml^{-1}; and Abcam[30]; rabbit IgG raised against extracellular residues 1–416; final concentration of 0.5 μg ml^{-1}). As controls for specificity, we used the corresponding class-matched antibodies (goat IgG, Pierce; rabbit IgG, Pierce; mouse IgG, Pierce; or chicken IgY, Promega) for comparison. The class-matched controls for the midkine, TrkB and TrkA antibodies were the goat IgG (4 μg ml^{-1}), mouse IgG (4 μg ml^{-1}) and rabbit IgG (2 μg ml^{-1}). The class-matched controls for the BDNF and PTPζ antibodies were the rabbit IgG and chicken IgY, used at 2 μg ml^{-1} and 10 μg ml^{-1}, respectively. The class-matched control for the FGF-1 antibody was the mouse IgG, used at 4 μg ml^{-1}. We cultured neurons for an additional 24 h before immunostaining them with an antibody to tubulin (Sigma; 1:500) and analyzing them by microscopy. We determined the relative concentrations of the CS tetrasaccharides by measuring the uronic acid content using the carbazole reaction as described previously[14].

Note: Supplementary information is available on the Nature Chemical Biology website.

ACKNOWLEDGMENTS

We thank V.W.T. Kam for assistance with modifying the Dreiding force field; R.H. Grubbs for the catalyst; C.J. Rogers for assistance with data analysis; J.L. Riechmann, director of the Millard and Muriel Jacobs Genetic and Genomics Laboratory at Caltech, for assistance with printing the microarrays; S. Ou in the Caltech Monoclonal Antibody Facility; and the Biological Imaging Center and Environmental Analysis Center at Caltech for instrumentation. This work was supported by the American Cancer Society (RSG-05-106-01-CDD), Human Frontiers Science Program, Tobacco-Related Disease Research Program (14RT-0034), National Institutes of Health (RO1 NS045061, C.I.G. and L.C.H.-W.), National Science Foundation (S.E.T.) and Howard Hughes Medical Institute.

AUTHOR CONTRIBUTIONS

C.I.G. and S.E.T. contributed equally to this work.

COMPETING INTERESTS STATEMENT

The authors declare that they have no competing financial interests.

Published online at http://www.nature.com/naturechemicalbiology
Reprints and permissions information is available online at http://npg.nature.com/reprintsandpermissions/

1. Hacker, U., Nybakken, K. & Perrimon, N. Heparan sulphate proteoglycans: the sweet side of development. *Nat. Rev. Mol. Cell Biol.* **6**, 530–541 (2005).
2. Capila, I. & Linhardt, R.J. Heparin-protein interactions. *Angew. Chem. Int. Edn Engl.* **41**, 391–412 (2002).
3. Sasisekharan, R., Shriver, Z., Venkataraman, G. & Narayanasami, U. Roles of heparan-sulphate glycosaminoglycans in cancer. *Nat. Rev. Cancer* **2**, 521–528 (2002).
4. Bradbury, E.J. *et al.* Chondroitinase ABC promotes functional recovery after spinal cord injury. *Nature* **416**, 636–640 (2002).
5. Kitagawa, H., Tsutsumi, K., Tone, Y. & Sugahara, K. Developmental regulation of the sulfation profile of chondroitin sulfate chains in the chicken embryo brain. *J. Biol. Chem.* **272**, 31377–31381 (1997).
6. Plaas, A.H.K., West, L.A., Wong-Palms, S. & Nelson, F.R.T. Glycosaminoglycan sulfation in human osteoarthritis. Disease-related alterations at the non-reducing termini of chondroitin and dermatan sulfate. *J. Biol. Chem.* **273**, 12642–12649 (1998).
7. Holt, C.E. & Dickson, B.J. Sugar codes for axons? *Neuron* **46**, 169–172 (2005).
8. Nandini, C.D. *et al.* Structural and functional characterization of oversulfated chondroitin sulfate/dermatan sulfate hybrid chains from the notochord of hagfish. Neuritogenic and binding activities for growth factors and neurotrophic factors. *J. Biol. Chem.* **279**, 50799–50809 (2004).
9. Ueoka, C. *et al.* Neuronal cell adhesion, mediated by the heparin-binding neuroregulatory factor midkine, is specifically inhibited by chondroitin sulfate E. Structural and functional implications of the over-sulfated chondroitin sulfate. *J. Biol. Chem.* **275**, 37407–37413 (2000).
10. Shuo, T. *et al.* Developmental changes in the biochemical and immunological characters of the carbohydrate moiety of neuroglycan C, a brain-specific chondroitin sulfate proteoglycan. *Glycoconj. J.* **20**, 267–278 (2004).
11. Tsuchida, K. *et al.* Appican, the proteoglycan form of the amyloid precursor protein, contains chondroitin sulfate E in the repeating disaccharide region and 4-*O*-sulfated galactose in the linkage region. *J. Biol. Chem.* **276**, 37155–37160 (2001).
12. Deepa, S.S., Yamada, S., Zako, M., Goldberger, O. & Sugahara, K. Chondroitin sulfate chains on syndecan-1 and syndecan-4 from normal murine mammary gland epithelial cells are structurally and functionally distinct and cooperate with heparan sulfate chains to bind growth factors. A novel function to control binding of midkine, pleiotrophin, and basic fibroblast growth factor. *J. Biol. Chem.* **279**, 37368–37376 (2004).
13. Karst, N.A. & Linhardt, R.J. Recent chemical and enzymatic approaches to the synthesis of glycosaminoglycan oligosaccharides. *Curr. Med. Chem.* **10**, 1993–2031 (2003).
14. Tully, S.E. *et al.* A chondroitin sulfate small molecule that stimulates neuronal growth. *J. Am. Chem. Soc.* **126**, 7736–7737 (2004).
15. Jacquinet, J.-C., Rochepeau-Jobron, L. & Combal, J.-P. Multigram syntheses of the disaccharide repeating units of chondroitin 4- and 6-sulfates. *Carbohydr. Res.* **314**, 283–288 (1998).
16. Brickman, Y.G. *et al.* Structural modification of fibroblast growth factor-binding heparan sulfate at a determinative stage of neural development. *J. Biol. Chem.* **273**, 4350–4359 (1998).
17. Kantor, D.B. *et al.* Semaphorin 5A is a bifunctional axon guidance cue regulated by heparan and chondroitin sulfate proteoglycans. *Neuron* **44**, 961–975 (2004).
18. Mayo, S.L., Olafson, B.D. & Goddard, W.A., III DREIDING: A generic force field for molecular simulations. *J. Phys. Chem.* **94**, 8897–8909 (1990).

© 2006 Nature Publishing Group http://www.nature.com/naturechemicalbiology

19. Rappe, A.K. & Goddard, W.A., III Charge equilibration for molecular dynamics simulations. *J. Phys. Chem.* **95**, 3358–3363 (1991).
20. Lim, K.-T. *et al.* Molecular dynamics for very large systems on massively parallel computers: the MPSim program. *J. Comput. Chem.* **18**, 501–521 (1997).
21. Feizi, T., Fazio, F., Chai, W. & Wong, C.H. Carbohydrate microarrays—a new set of technologies at the frontiers of glycomics. *Curr. Opin. Struct. Biol.* **13**, 637–645 (2003).
22. de Paz, J.L., Noti, C. & Seeberger, P.H. Microarrays of synthetic heparin oligosaccharides. *J. Am. Chem. Soc.* **128**, 2766–2767 (2006).
23. Park, S., Lee, M.R., Pyo, S.J. & Shin, I. Carbohydrate chips for studying high-throughput carbohydrate-protein interactions. *J. Am. Chem. Soc.* **126**, 4812–4819 (2004).
24. Muramatsu, T. Midkine and pleiotrophin: two related proteins involved in development, survival, inflammation and tumorigenesis. *J. Biochem.* **132**, 359–371 (2002).
25. Herndon, M.E., Stipp, C.S. & Lander, A.D. Interactions of neural glycosaminoglycans and proteoglycans with protein ligands: assessment of selectivity, heterogeneity and the participation of core proteins in binding. *Glycobiology* **9**, 143–155 (1999).
26. Huang, E.J. & Reichardt, L.F. Neurotrophins: roles in neuronal development and function. *Annu. Rev. Neurosci.* **24**, 677–736 (2001).
27. Bicknese, A.R., Sheppard, A.M., O'Leary, D.D. & Pearlman, A.L. Thalamocortical axons extend along a chondroitin sulfate proteoglycan-enriched pathway coincident with the neocortical subplate and distinct from the efferent path. *J. Neurosci.* **14**, 3500–3510 (1994).
28. Jiang, B., Akaneya, Y., Hata, Y. & Tsumoto, T. Long-term depression is not induced by low-frequency stimulation in rat visual cortex *in vivo*: a possible preventing role of endogenous brain-derived neurotrophic factor. *J. Neurosci.* **23**, 3761–3770 (2003).
29. Seil, F.J. & Drake-Baumann, R. TrkB receptor ligands promote activity-dependent inhibitory synaptogenesis. *J. Neurosci.* **20**, 5367–5373 (2000).
30. Skoff, A.M. & Adler, J.E. Nerve growth factor regulates substance P in adult sensory neurons through both TrkA and p75 receptors. *Exp. Neurol.* **197**, 430–436 (2006).
31. Bellaiche, Y., The, I. & Perrimon, N. *Tout-velu* is a *Drosophila* homologue of the putative tumour suppressor *EXT-1* and is needed for Hh diffusion. *Nature* **394**, 85–88 (1998).
32. Fernaud-Espinosa, I., Nieto-Sampedro, M. & Bovolenta, P. Developmental distribution of glycosaminoglycans in embryonic rat brain: relationship to axonal tract formation. *J. Neurobiol.* **30**, 410–424 (1996).
33. Greeley, B.H. *et al.* New pseudospectral algorithms for electronic structure calculations: length scale separation and analytical two-electron integral corrections. *J. Chem. Phys.* **101**, 4028–4041 (1994).

© 2006 Nature Publishing Group http://www.nature.com/naturechemicalbiology